

Supplementary Material and Methods

NMR Spectroscopy

Protein purification. Talin1-F0 (1-86) subcloned into a pHis-1 vector¹ was used as a template to generate Talin1-F0 single mutants including K15A, R35A and R35E by using QuickChange lightning site-directed mutagenesis Kit (Agilent Technologies). Talin1-F0_DM (K15A, R35A) subcloned into a pHis-1 vector¹ was used as a template to generate Talin1-F0_3mut (K15A, R30A, R35A) using the same mutagenesis Kit. Talin1-F0 (WT or mutant) was expressed in *E.coli* BL21 (DE3) strain and ¹⁵N Isotope-labeled Talin1-F0 was achieved by growing bacteria in minimal medium with ¹⁵NH₄Cl as the sole nitrogen source. Talin1-F0 was first purified by nickel affinity column and then incubated with TEV protease to remove the recombinant N-terminal 6xHis-tag. By flowing through nickel affinity column, untagged Talin1-F0 was collected and subjected to gel filtration by using Superdex-75 (10/300, GE Healthcare), which was pre-equilibrated with buffer containing 20 mM NaH₂PO₄/Na₂HPO₄ (pH 6.6), 50 mM NaCl and 2 mM Dithiothreitol (DTT). Protein concentration was measured by absorbance at 280 nm. Human full-length Rap1b (G12V) subcloned into a pET28a vector¹ was used to express active form of Rap1b. Rap1b (G12V) with N-terminal 6xHis tag was purified by nickel affinity column, followed by anion exchange using Hi-trap Q column (GE Healthcare). Gel filtration was performed in the final step by using Superdex-75 (16/60, GE Healthcare). Purified Rap1b (G12V) was then loaded with Guanosine 5'-[β, γ-imido] triphosphate trisodium salt (GMP-PNP)¹ for experiment use. Protein concentration of Rap1b (G12V) was measured by Pierce 660 nm protein assay reagent (Thermo Fisher Scientific).

NMR 2D-HSQC. HSQC experiments were performed on a Bruker 600 or 700 MHz NMR spectrometer. Samples containing ¹⁵N-labeled Talin1-F0 (WT or mutant) in the absence or presence of GMP-PNP loaded Rap1b (G12V) were studied. Experiments were performed at 25 °C in buffer containing 20 mM NaH₂PO₄/Na₂HPO₄ (pH 6.6), 50 mM NaCl, 5 mM MgCl₂, 2 mM Dithiothreitol (DTT) and 5% D₂O. Chemical shift change ($\Delta\delta_{\text{obs}}_{[\text{HN},\text{N}]}$) of each selected residue was calculated with the equation $\Delta\delta_{\text{obs}}_{[\text{HN},\text{N}]} = [(\Delta\delta_{\text{HN}}W_{\text{HN}})^2 + (\Delta\delta_{\text{N}}W_{\text{N}})^2]^{1/2}$ where $\Delta\delta$ (ppm) = $\delta_{\text{bound}} - \delta_{\text{free}}$, and W_{HN} and W_{N} are weighting factors, $W_{\text{HN}} = 1$, $W_{\text{N}} = 0.154$.

Antibodies and reagents

The following antibodies were used for flow cytometry: FITC-labeled hamster IgM anti-CD29 (Biolegend, Uithoorn, Netherlands), rat IgG2a anti-CD18, hamster IgG anti-CD61, hamster IgG anti-CD49b, rat IgG2a anti-CD41, rat IgG2a anti-CD49e (BD Biosciences, Heidelberg, Germany),

isotype controls rat IgG (Thermo Fisher Scientific, Braunschweig, Germany) and hamster IgG (BD Biosciences, Heidelberg, Germany), PE-labeled rat IgG2b anti-activated integrin α IIb β 3 clone JON/A (Emfret Analytics, Eibelstadt, Germany), fibrinogen-Alexa Fluor 647, Phalloidin-Alexa Fluor 546, eFluor450-labeled rat IgG2b anti-CD11b and biotinylated rat IgG2b anti-Ly-6G (Gr-1) (Thermo Fisher Scientific), Streptavidin-Cy5 (Jackson ImmunoResearch Laboratories, Inc.; Suffolk; UK). All flow cytometry based assays were carried out using an LSRFortessa™ X-20 flow cytometer (BD Biosciences). The following antibodies were used for Western blotting: mouse anti-Talin, mouse anti-Actin (Sigma-Aldrich, Deisenhofen, Germany), rabbit anti-RIAM (Abcam, Cambridge, UK), rabbit anti-Talin1 (Cell Signaling Technology, Frankfurt, Germany), mouse anti-Talin2 (Abcam plc, Cambridge, UK) rabbit anti-Rap1 (Santa Cruz Biotechnology, Inc., Heidelberg, Germany), rabbit anti-Kindlin-3 (homemade²), mouse anti-GAPDH (Merck-Millipore, Darmstadt, Germany), goat anti-rabbit-HRP and goat anti-mouse-HRP (Jackson ImmunoResearch Laboratories). Antibodies used for immunofluorescence stainings: mouse anti-Talin2, rabbit anti-Paxillin (both Abcam plc), rat anti-active β 1 integrin (9EG7; BD Pharmingen), rabbit anti- β 1 integrin (homemade³), goat anti-mouse-Cy3 (Jackson ImmunoResearch Laboratories), goat anti-rabbit-Alexa Fluor 488, goat anti-rat-Alexa Fluor 546 and Phalloidin-Alexa Fluor 647 (Thermo Fisher Scientific).

The following agonists were used for platelet studies: Chrono-Par-Thrombin, Chrono-Par-ADP, Chrono-Par-Collagen (Probe & go Labordiagnostica GmbH, Lemgo, Germany), U46619 (Enzo Life Sciences GmbH, Lörrach, Germany) and Collagen-related peptide (CRP; kindly provided by Prof. Siess, LMU, Munich). The following ligands and agonists were used for leukocyte studies: recombinant human ICAM-1, recombinant human VCAM-1 (both R&D Systems, Abingdon, UK), fibronectin (Sigma-Aldrich), vitronectin (STEMCELL Technologies, Köln, Germany), PMA (Merck-Millipore), TNF- α (R&D Systems).

Platelet integrin activation, aggregation and spreading

Platelet *in vitro* assays were either performed on isolated platelets or whole blood samples. Platelet preparation was performed by repeated centrifugation of heparinized blood at 50 g for 5 min and harvesting the upper platelet containing fraction. Platelets were washed in Tyrode's buffer (136 mM NaCl, 0.43 mM NaH₂PO₄, 2.7 mM KCl, 12mM NaHCO₃, 5 mM HEPES, 0.1% glucose, 0.35% BSA; pH 7.35) containing apyrase and PGI₂ and kept at 37 °C. Platelet concentration was measured using a ProCyte Dx Hematology Analyzer (IDEXX, Westbrook, USA).

Integrin activation and platelet aggregation⁴, platelet spreading⁵ and platelet filamentous actin content measurement⁶ were in essence carried out as previously described.

Integrin activation was assessed on heparinized blood samples washed twice with Tyrode's buffer and resuspended in Tyrode's buffer containing 2 mM CaCl₂ and 1 mM MgCl₂. Platelets were stimulated with indicated agonists and stained either with JON/A-PE antibody or AlexaFluor 647-labeled fibrinogen for 15 min at 37 °C. Active integrin level was measured by flow cytometry using an LSRFortessa™ X-20 flow cytometer (BD Biosciences). An activation index was calculated by normalizing active integrin staining intensity to total integrin β3 levels.

For platelet aggregation studies, washed platelets were treated with indicated agonists in the presence of fibrinogen and light transmission was measured using a Chrono-Log aggregometer for 15 min.

Spreading assays were carried out on glass bottom microwell dishes (MatTek Corporation, Ashland, USA) coated with 200 µg/ml fibrinogen (Sigma-Aldrich) over night. After blocking with 1% BSA/PBS for 30 min, 10⁷ platelets were seeded upon stimulation with 0.01 U/ml thrombin. Adherent platelets were fixed with 4% paraformaldehyde (PFA) at indicated time points and imaged using an Eclipse Ti live cell microscope equipped with a 100x NA 1.45 Plan Apo λ objective (Nikon Instruments, Amsterdam, Netherlands) and a ProEM EMCCD Camera (Princeton Instruments). Platelet spreading area and stage of spreading were analyzed using ImageJ software (US National Institutes of Health).

Leukocyte adhesion and spreading assays

Neutrophil and macrophage adhesion and spreading assays were performed as previously described⁷. For adhesion assays, non-cell culture-treated 96-well plates were coated with recombinant human ICAM-1 (4 µg/ml), VCAM-1 (4 µg/ml), vitronectin (2.5 µg/ml) or fibronectin (5 µg/ml) in coating buffer (20 mM Tris-HCl pH 9.0, 150 mM NaCl, 2 mM MgCl₂) at 4 °C overnight. Plates were washed with PBS and blocked with 3% BSA. PMNs were isolated from bone marrow and 5 x 10⁴ cells / well were seeded in adhesion medium (RPMI1640 containing 0.1% fetal bovine serum) in the absence or presence of PMA or TNF-α. For measurement of macrophage adhesion, an equal number of cells was seeded. After 30 min, plates were washed with PBS and adherent cells fixed with 4% PFA for 15 min. PMNs were stained with DAPI and imaged using an Evos FL Auto 2 live cell microscope (Thermo Fisher Scientific). Adherent cells were counted using ImageJ software. Adherent macrophages were stained with 5 mg/ml crystal violet in 2% ethanol. After washing the plates, remaining dye was solved in 2% SDS and quantified using a plate reader (Tecan, Männedorf, Switzerland).

Macrophage spreading was analyzed on fibronectin (5 µg/ml) or ICAM-1 (4 µg/ml) coated surfaces. Phase contrast images were taken 15, 30, 60 and 120 min after plating the cells using an Evos FL Auto 2 life cell microscope and spreading areas of 20 cells per time point, coating and group were measured using ImageJ software.

Macrophage β 1 integrin activation was assessed by 9EG7 staining. Bone marrow derived macrophages were seeded on fibronectin-coated (5 µg/ml) glass coverslips (Thermo Fisher Scientific) in adhesion medium (RPMI 1640 containing 0.1% fetal bovine serum) for 2 h. Cells were washed with PBS, stained with active β 1 integrin specific 9EG7 antibody for 30 min and fixed with 4% PFA. Cells were further stained using rabbit anti-integrin β 1, goat anti-rat-Alexa Fluor 546 and goat anti-rabbit-Alexa Fluor 488 and imaged using a Leica TCS SP5 X confocal microscope (Leica Microsystems, Wetzlar, Germany). Staining intensities of 9EG7 and total β 1 staining were analyzed in areas of clustered integrins using ImageJ software.

Neutrophil phagocytosis assay

The neutrophil phagocytosis assay was performed using a pHrodo™ Red E. coli BioParticles™ Phagocytosis Kit for Flow Cytometry (Thermo Fisher Scientific) following the manufacturers' instructions. The relative amount of phagocytosed *Escherichia coli* particles was assessed by flow cytometry using an LSRFortessa™ X-20 flow cytometer (BD Biosciences).

Adhesion, spreading and focal adhesion analysis of primary and Talin^{1/2dko} fibroblasts

Primary mouse embryonic fibroblasts derived from WT and *Tln1*^{3mut} E14.5 embryos and Talin^{1/2dko} fibroblasts were cultured in DMEM GlutaMAX™ supplemented with 10% fetal bovine serum, non-essential amino acids, 100 U/ml penicillin and 100 µg/ml streptomycin (all Thermo Fisher Scientific) under standard conditions.

To compare effects of a double (K15A, R35A; Talin DM) or triple (K15A, R30A, R35A; Talin 3mut) mutation in Talin1-F0, ypet-tagged WT Talin1, Talin1 DM, Talin1 3mut and Talin1 Δ F0 were expressed in murine Talin^{1/2dko} fibroblasts and cell adhesion, spreading and Talin1 recruitment to focal adhesions were analyzed as previously described¹.

To analyze focal adhesions in mouse embryonic fibroblasts, cells were cultured on fibronectin-coated (5 µg/ml) coverslips for 4 h and fixed with 4% PFA for 10 min. Cells were stained using mouse anti-Talin2, rabbit anti-Paxillin, goat anti-mouse-Cy3 and goat anti-rabbit-Alexa Fluor 488 and imaged using a Leica TCS SP5 X confocal microscope. Focal adhesions were quantified by measuring Paxillin positive areas using ImageJ software.

1. Zhu L, Yang J, Bromberger T, et al. Structure of Rap1b bound to talin reveals a pathway for triggering integrin activation. *Nat Commun.* 2017;8(1):1744.
2. Ussar S, Wang HV, Linder S, Fassler R, Moser M. The Kindlins: subcellular localization and expression during murine development. *Exp Cell Res.* 2006;312(16):3142-3151.
3. Azimifar SB, Bottcher RT, Zanivan S, et al. Induction of membrane circular dorsal ruffles requires co-signalling of integrin-ILK-complex and EGF receptor. *J Cell Sci.* 2012;125(Pt 2):435-448.
4. Klapproth S, Moretti FA, Zeiler M, et al. Minimal amounts of kindlin-3 suffice for basal platelet and leukocyte functions in mice. *Blood.* 2015;126(24):2592-2600.
5. Hofmann S, Braun A, Pozgaj R, Morowski M, Vogtle T, Nieswandt B. Mice lacking the SLAM family member CD84 display unaltered platelet function in hemostasis and thrombosis. *PLoS One.* 2014;9(12):e115306.
6. Petzold T, Ruppert R, Pandey D, et al. beta1 integrin-mediated signals are required for platelet granule secretion and hemostasis in mouse. *Blood.* 2013;122(15):2723-2731.
7. Klapproth S, Sperandio M, Pinheiro EM, et al. Loss of the Rap1 effector RIAM results in leukocyte adhesion deficiency due to impaired beta2 integrin function in mice. *Blood.* 2015;126(25):2704-2712.

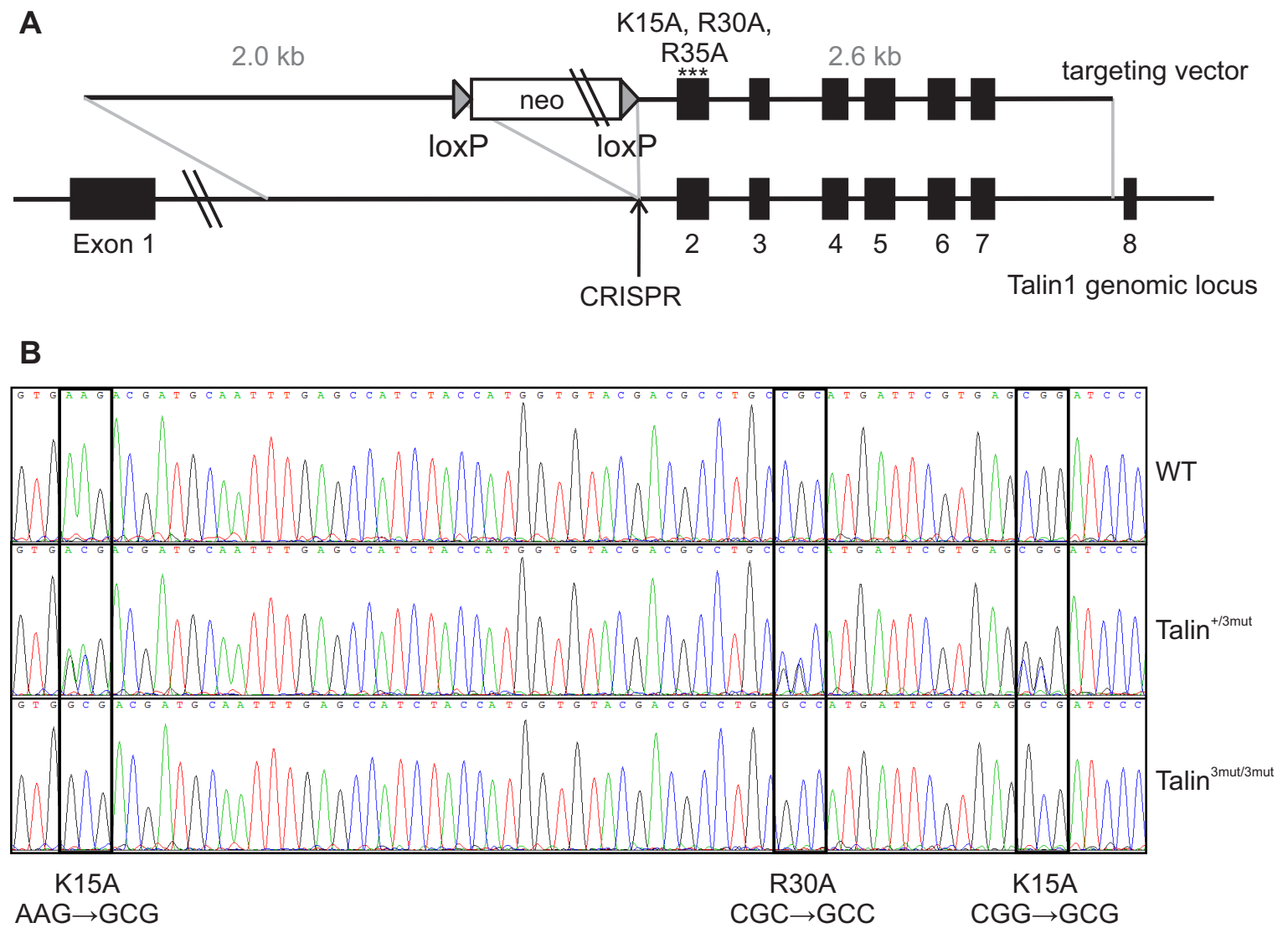
Supplementary Table 1: Genotypes of offspring from heterozygous $Tln1^{3mut}$ intercrosses.

	Animal count	Ratio [%]
Talin^{+/+}	62	26.2
Talin^{+/3mut}	115	48.5
Talin^{3mut/3mut}	60	25.3
Σ	237	100

Supplementary Table 2: Peripheral blood cell counts of WT and $Tln1^{3mut}$ mice (N=14/15). Values are given as mean \pm 95% CI.

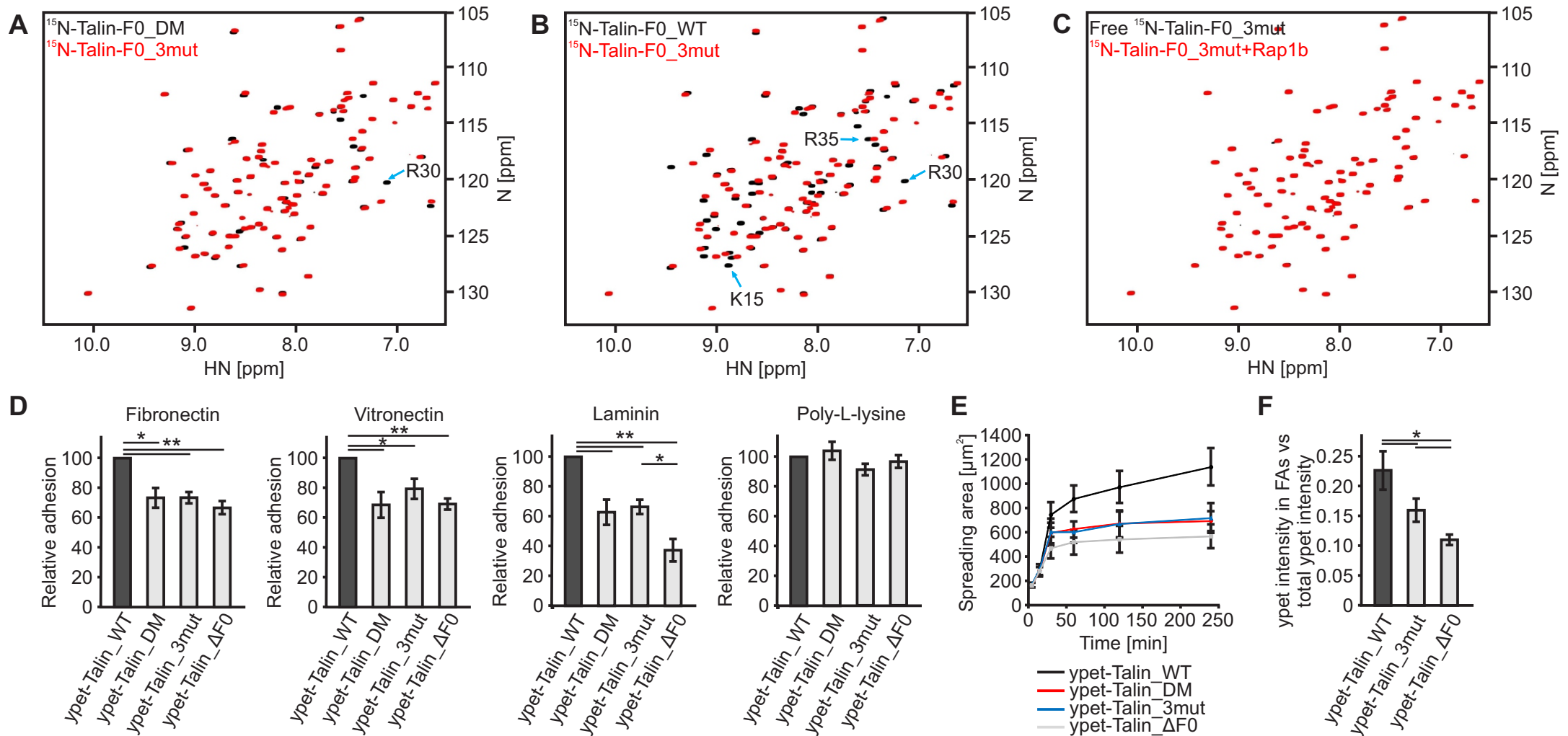
	WT (n=14)	Talin^{3mut} (n=15)
Platelets [K/μL]	626 \pm 58	577 \pm 57
Mean platelet volume [fL]	5.77 \pm 0.14	5.70 \pm 0.25
White blood cells [K/μL]	8.46 \pm 1.33	9.37 \pm 1.73
Neutrophils [K/μL]	1.04 \pm 0.26	1.20 \pm 0.34
Lymphocytes [K/μL]	7.17 \pm 1.19	7.90 \pm 1.44
Monocytes [K/μL]	0.12 \pm 0.05	0.13 \pm 0.05
Eosinophils [K/μL]	0.12 \pm 0.04	0.13 \pm 0.07
Basophils [K/μL]	0.01 \pm 0.01	0.01 \pm 0.00
Red blood cells [M/μL]	10.02 \pm 0.24	10.04 \pm 0.26
Hemoglobin, [g/dL]	15.26 \pm 0.24	15.29 \pm 0.36
Hematocrit [%]	49.16 \pm 0.99	49.05 \pm 1.27

Supplementary Figure 1



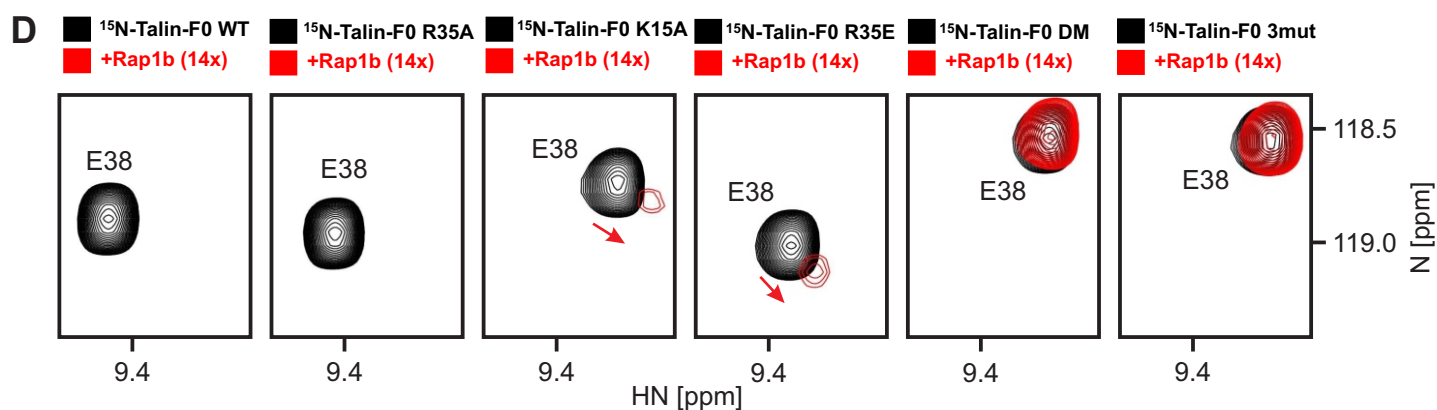
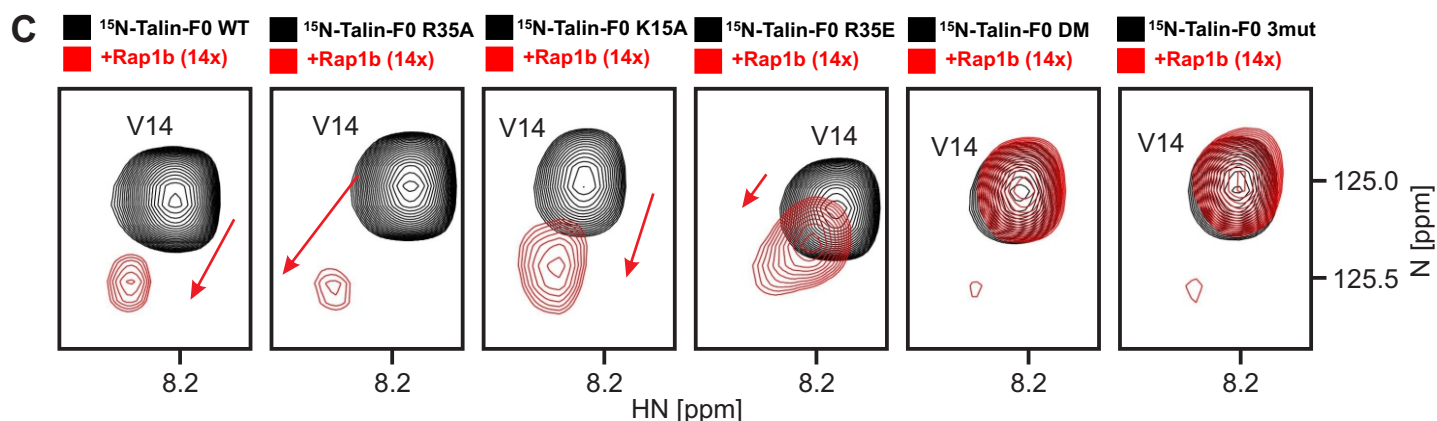
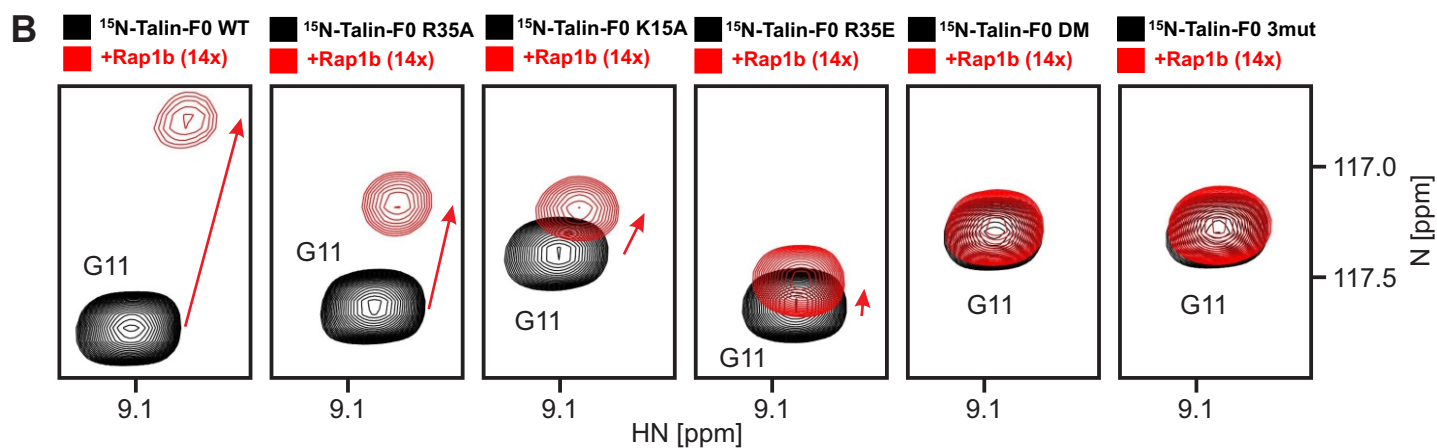
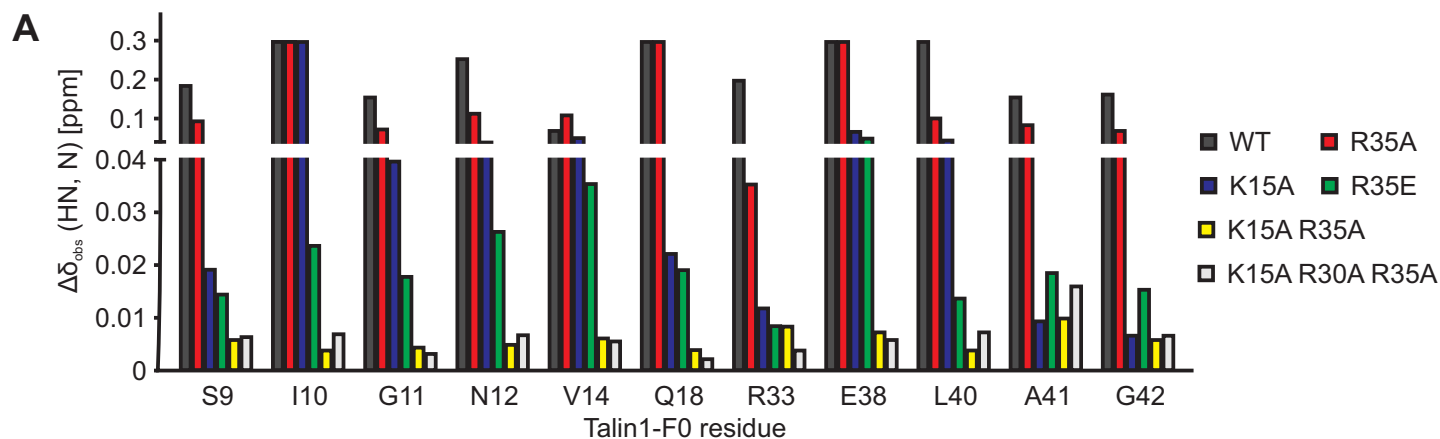
Supplementary Figure 1: Generation of *Tln1*^{3mut} mice. (A) Targeting strategy of the Talin1 gene locus. Partial map of the Talin1 gene and the targeting vector, which carries mutations in exon 2 leading to the indicated amino acid substitutions. The targeting vector contains a neomycin-resistance cassette, which was later removed by breeding mice with a deleter-Cre strain. (B) Exon 2 from control, heterozygous and homozygous *Tln1*^{3mut} mice was amplified by genomic PCR and sequenced. The three mutations are marked in the sequencing histograms.

Supplementary Figure 2



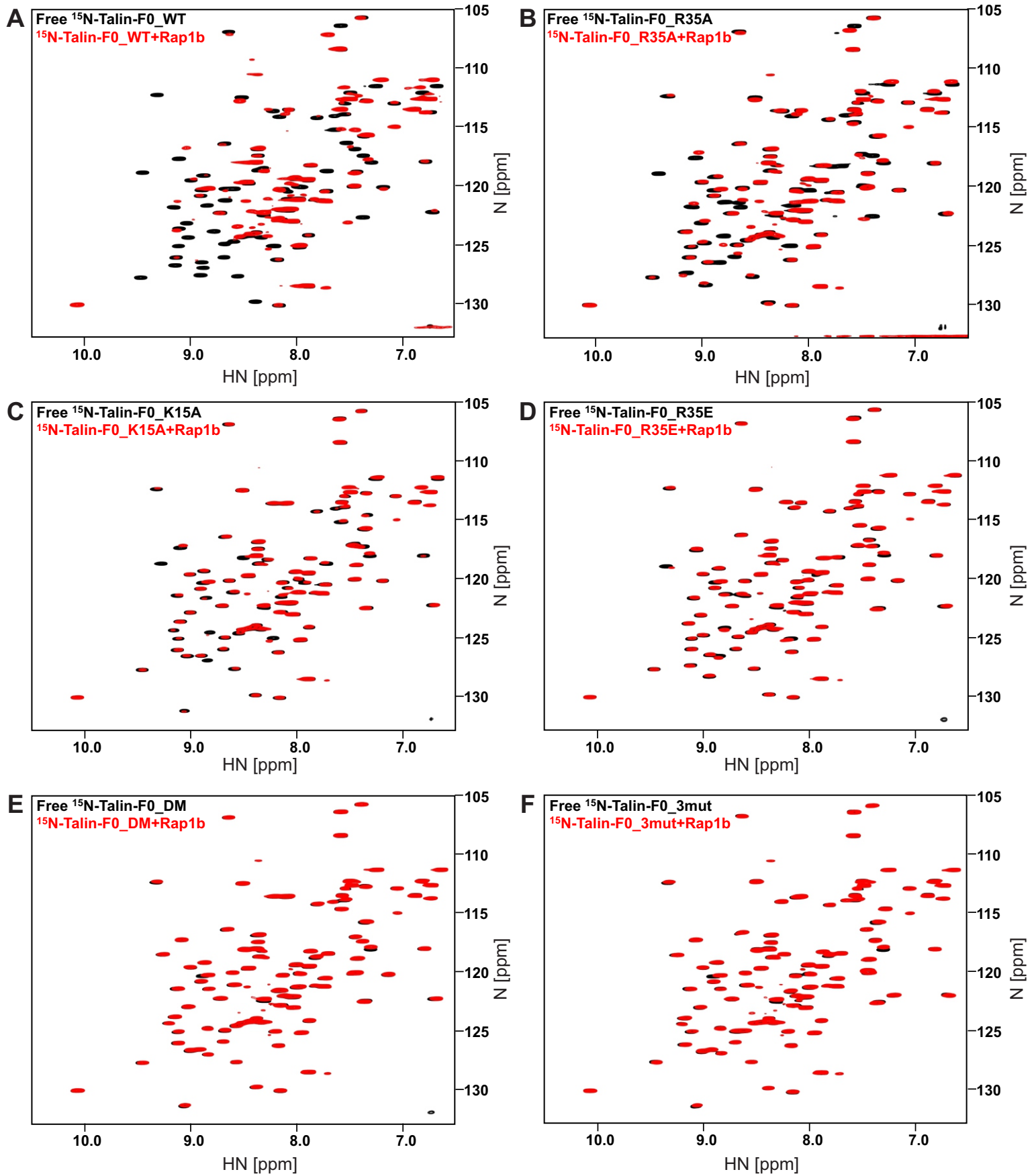
Supplementary Figure 2: Triple mutation (3mut; K15A, R30A, R35A) in Talin1-F0 disrupted the Talin1-F0/Rap1 interaction and generates equal effects as a double mutation (DM; K15A, R35A). (A) HSQC spectral overlay of 50 μM ^{15}N -labeled Talin1-F0_DM (black) and Talin1-F0_3mut (red). (B) HSQC spectral overlay of 50 μM ^{15}N -labeled Talin1-F0_WT (black) and Talin1-F0_3mut (red). (C) The HSQC spectra of 50 μM ^{15}N -labeled Talin1-F0_3mut in the absence (black) and presence of 125 μM GMP-PNP loaded Rap1b (red). (D) Static adhesion of Talin^{1/2dko} fibroblasts expressing ypet-tagged Talin1_DM, Talin1_3mut or Talin1_ ΔF0 relative to cells expressing ypet-tagged WT Talin1 on fibronectin, vitronectin, laminin and poly-L-lysine coated surfaces (N=5 experiments). (E) Spreading of Talin^{1/2dko} fibroblasts expressing ypet-tagged WT Talin1, Talin1_DM, Talin1_3mut or Talin1_ ΔF0 assessed 5, 15, 30, 60, 120 and 240 min after seeding the cells on a fibronectin coated surface (N=4 experiments). (F) Talin1 recruitment in Talin1_WT, Talin1_3mut and Talin1_ ΔF0 rescued Talin^{1/2dko} fibroblasts assessed by measuring ypet intensity in focal adhesions normalized against ypet intensity of whole cells (N=3 experiments). All values are given as mean \pm SEM, * p < 0.05, ** p < 0.01.

Supplementary Figure 3



Supplementary Figure 3: Talin1-F0 double (DM; K15A, R35A) or triple mutant (3mut; K15A, R30A, R35A) showed further reduced binding to Rap1b compared to single mutants. (A) Chemical shift changes of 70 μM ^{15}N -labeled Talin1-F0 WT and mutants including V14, R35A, K15A, R35E, K15A/R35A (DM) and K15A/R30A/R35A (3mut) induced by the presence of 1 mM GMP-PNP loaded Rap1b (G12V). Interface residues indicated in the figure were analyzed. Chemical shift changes of broader residues were set to 0.3. The data suggest that compared to Talin1-F0 single mutants, DM or 3mut are more potent in disrupting Talin1-F0/Rap1b interaction. (B-D) Spectra of representative residues, Glycine 11 (B), Valine 14 (C) and Glutamate 38 (D) of indicated Talin1-F0 variants in the absence (black) and presence (red) of GMP-PNP loaded Rap1b (G12V).

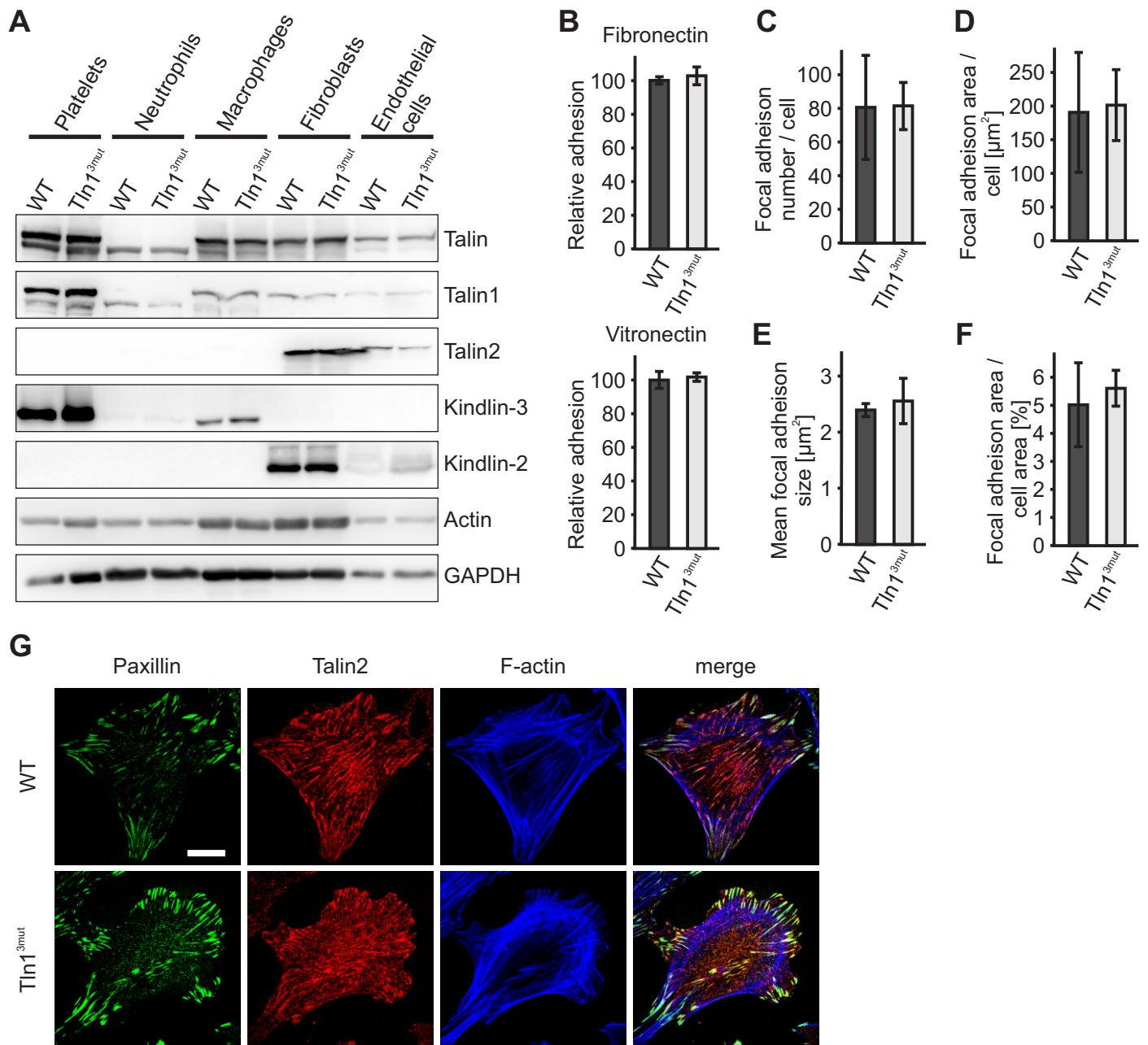
Supplementary Figure 4



Supplementary Figure 4: Comparison of Rap1b binding to different Talin1-F0 variants by NMR HSQC.

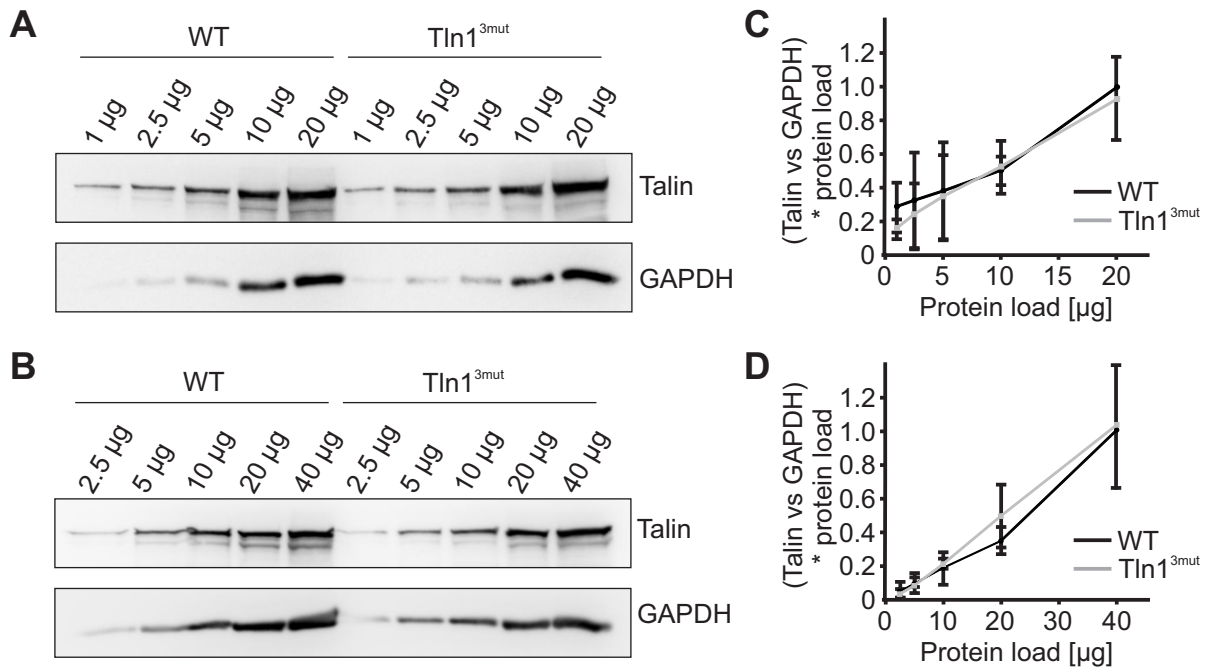
(A-F) Full HSQC spectra of $70\ \mu\text{M}$ ^{15}N -labeled Talin1-F0 WT (A), R35A (B), K15A (C), R35E (D), K15A/R35A (DM) (E) and K15A/R30A/R35A (3mut) (F) in the absence (black) and presence (red) of 1 mM GMP-PNP loaded Rap1b.

Supplementary Figure 5



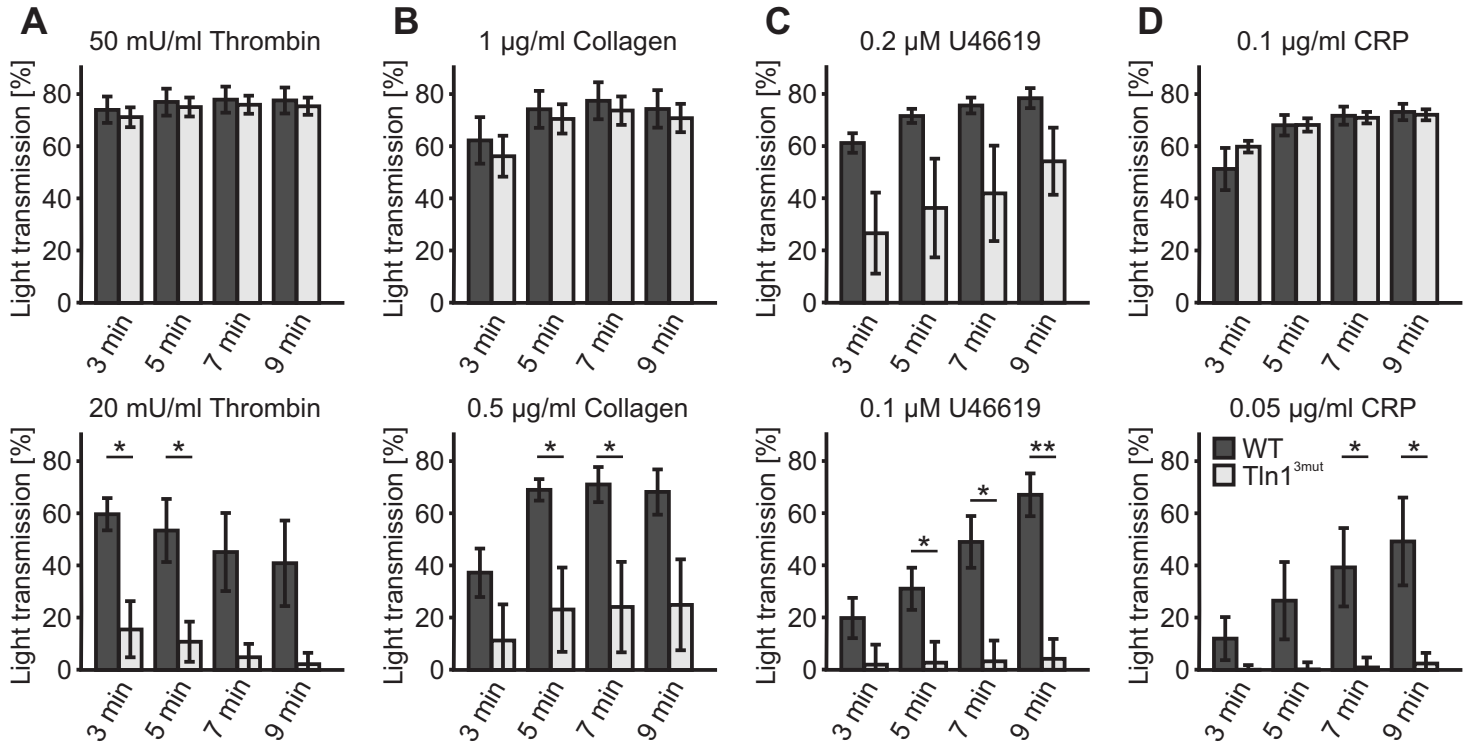
Supplementary Figure 5: Adhesion and focal adhesion formation is not altered in Tln1^{3mut} fibroblasts. (A) Total Talin, Talin1, Talin2, Kindlin-2 and Kindlin-3 expression in platelets, neutrophils, macrophages, fibroblasts and endothelial cells analyzed by Western blotting. Actin and GAPDH served as loading controls. (B) Static adhesion of WT and Tln1^{3mut} embryonic fibroblasts on fibronectin and vitronectin (N=6; cells isolated from 3 embryos per genotype). (C-F) Paxillin was immunofluorescently labeled in WT and Tln1^{3mut} mouse embryonic fibroblasts plated on fibronectin-coated surfaces. Focal adhesion number (C), focal adhesion area per cell (D), mean focal adhesion size (E) and focal adhesion area relative to cell area (F) were quantified by counting and measuring Paxillin positive areas (N=5 experiments). (G) Immunofluorescence images of WT and Tln1^{3mut} embryonic fibroblasts showing Paxillin (green) as a focal adhesion marker, Talin2 (red) and F-actin (blue). Scale bar: 20 μm. All values are given as mean ± 95% CI.

Supplementary Figure 6



Supplementary Figure 6: Comparable Talin1 expression in WT and Tln1^{3mut} mice. (A, B) Talin expression in WT and Tln1^{3mut} platelets (A) and macrophages (B) analyzed by Western blotting. Increasing amounts of protein lysates were analyzed. GAPDH served as loading control. (C, D) Quantitative analysis of Western blots shown in (A) and (B) (value for highest amount of WT lysate set to 1). Values are given as mean \pm 95% CI (N=3).

Supplementary Figure 7



Supplementary Figure 7: Aggregation of Tln1^{3mut} platelets is affected at low agonist concentrations. (A-D) Quantification of platelet aggregation by measuring light transmission 3, 5, 7 and 9 min after activation with 50 or 20 mU/ml thrombin (A), 1 or 0.5 µg/ml collagen (B), 0.2 or 0.1 µM U46619 (C) and 0.1 or 0.05 µg/ml CRP (D) (N=4-5 mice). All values are given as mean ± SEM, * p<0.05, ** p<0.01.